3. OPERATION OF AXIAL FLOW FANS

3.1. Sources of losses

Turbomachinery blade passage flow: an interacting 3D flow phenomenon. In modern design methods, the losses are considered in their full complexity, with use of 3D computational fluid dynamics (CFD) simulations and measurements. It is still reasonable to categorize the loss sources in a classic way, for a deeper understanding of turbomachinery fluid dynamics. This classic categorization was formerly necessitated due to the limitations of measurement techniques and computational methods.

The following discussion is also valid for axial blowers and compressors.

3.1.1. Rotor blade profile losses (friction losses)

A percentage of the power necessary for rotating the rotor does work to win over the losses appearing due to the flow friction on the blades.

The most considerable portion of this loss appears in the decelerating region of the suction side boundary layer (**Fig. 3.1**). The thickening of the suction side boundary layer leads to the widening of the blade wake and thus, to the increase of blade drag.

The main goal of development of new efficient blade profiles – especially for compressors – is to minimise the losses in the decelerating region (Controlled Diffusion Airfoil, CDA, **Fig. 3.2**).

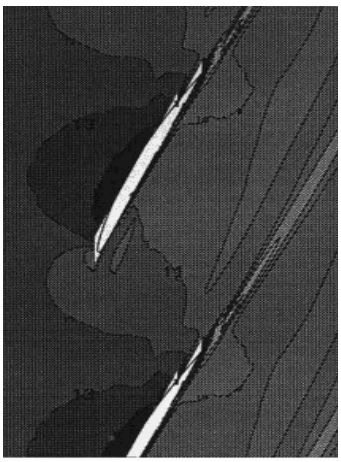

Fig. 3.1. Velocity distribution in the vicinity of an axial flow rotating blade row. Laser Doppler velocimeter measurements **[11]**

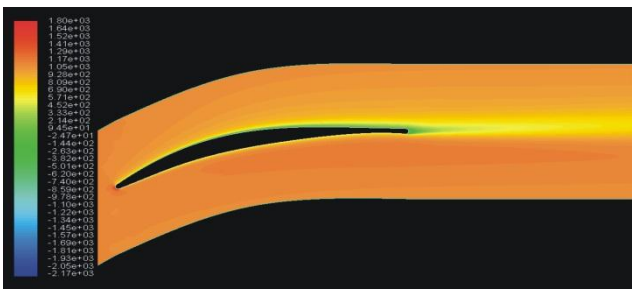

Fig. 3.2. Total pressure distribution computed in the vicinity of a CDA **[12]**

The drag appearing on an elemental blade section of height *dr* is

$$dF_D = \frac{\rho}{2} w_\infty^2 \; \ell \; dr \; c_D \tag{3.1}$$

This drag multiplied by the relative velocity in its direction gives the elemental power necessary to its being won over:

$$dP_R' = \frac{\rho}{2} w_\infty^3 \; \ell \; dr \; c_D \tag{3.2}$$

The integral of this elemental power along the radius gives the overall friction power of the rotor:

$$P_R' = N \frac{\rho}{2} \int_{r_{hub}}^{r_{tip}} w_\infty^3 \; \ell \; c_D dr \tag{3.3}$$

Which gives, divided by the total volume flow rate, the mean total pressure loss related to blade profile losses:

$$\Delta p_R' = \frac{N \frac{\rho}{2} \int_{r_{hub}}^{r_{tip}} w_\infty^3 \; \ell \; c_D dr}{\left(r_{tip}^2 - r_{hub}^2\right) \pi c_a} \tag{3.4}$$

In the next section, it is pointed out that the lift-to-drag ratio is to be maximised in order to minimise the profile losses. Let us multiply and also divide the function being integrated with the lift coefficient and the blade count:

$$\Delta p_R' = \frac{N \frac{\rho}{2} \int_{r_{hub}}^{r_{tip}} w_\infty^3 \frac{2r\pi}{N} \left(\frac{\ell}{t} c_L\right)\left(\frac{c_D}{c_L}\right) dr}{\left(r_{tip}^2 - r_{hub}^2\right) \pi c_a} = \frac{\rho \int_{r_{hub}}^{r_{tip}} w_\infty^3 \left(\frac{\ell}{t} c_L\right)\left(\frac{c_D}{c_L}\right) r \; dr}{\left(r_{tip}^2 - r_{hub}^2\right) c_a} \tag{3.5}$$

Considering that

$$\frac{\ell}{t} c_L \approx \frac{2 \, \Delta c_u}{w_\infty} = \frac{2 \Delta p_{tid}}{\rho u w_\infty} \tag{3.6a}$$

And $$w_\infty \approx u = r\omega \tag{3.6b}$$

$$\Delta p_R' = \frac{\rho \int_{r_{hub}}^{r_{tip}} w_\infty^3 \frac{2\Delta p_{tid}}{\rho u w_\infty} \left(\frac{c_D}{c_L}\right) r \; dr}{\left(r_{tip}^2 - r_{hub}^2\right) c_a} \approx \frac{2\Delta p_{tid} \omega \int_{r_{hub}}^{r_{tip}} \left(\frac{c_D}{c_L}\right) r^2 \; dr}{\left(r_{tip}^2 - r_{hub}^2\right) c_a} \tag{3.7}$$

This shows that the maximum of the lift-to-drag ratio gives the minimum profile losses indeed. Since the local values are to be weighted by the square of the radius, lift-to-drag values at the outer radii will mostly influence the rotor losses.

Taking the values at midspan as being representative along the entire span, the expression of pressure loss can be simplified as follows:

$$\Delta p_R' = \frac{N\frac{\rho}{2}\int_{r_{hub}}^{r_{tip}} w_\infty^3\, \ell\, c_D dr}{\left(r_{tip}^2 - r_{hub}^2\right)\pi c_a} \approx \frac{N\frac{\rho}{2} w_{\infty m}^3 \ell_m c_{Dm}\left(r_{tip} - r_{hub}\right)}{\left(r_{tip}^2 - r_{hub}^2\right)\pi c_a} = \frac{N\frac{\rho}{2} w_{\infty m}^3 \ell_m c_{Dm}}{\left(r_{tip} + r_{hub}\right)\pi c_a} =$$

$$= \frac{N\frac{\rho}{2} w_{\infty m}^3 \ell_m c_{Dm}}{2 r_m \pi c_a} = \frac{\rho}{2}\frac{w_{\infty m}^3}{c_a}\frac{\ell_m}{t_m} c_{Dm} \tag{3.8}$$

The profile loss relative to Δp_{tid} :

$$\frac{\Delta p_R'}{\Delta p_{tid}} = \frac{1}{\rho u_m \Delta c_{um}}\frac{\rho}{2}\frac{w_{\infty m}^3}{c_a}\frac{\ell_m}{t_m} c_{Dm} = \frac{w_{\infty m}}{u_m}\frac{1}{\sin\left(\beta_{\infty m} + \delta\right)}\frac{c_{Dm}}{c_{Lm}} \tag{3.9}$$

The transformation of the expression into this form is beneficial also because the other kinds of losses will be calculated at midspan as well.

The rotor profile losses contribute usually only some percents to the reduction of rotor hydraulic efficiency. **Fig. 3.3** shows the spanwise distribution of local hydraulic efficiency calculated from measurement data. Near midspan, the values of local hydraulic efficiency are above 95 %.

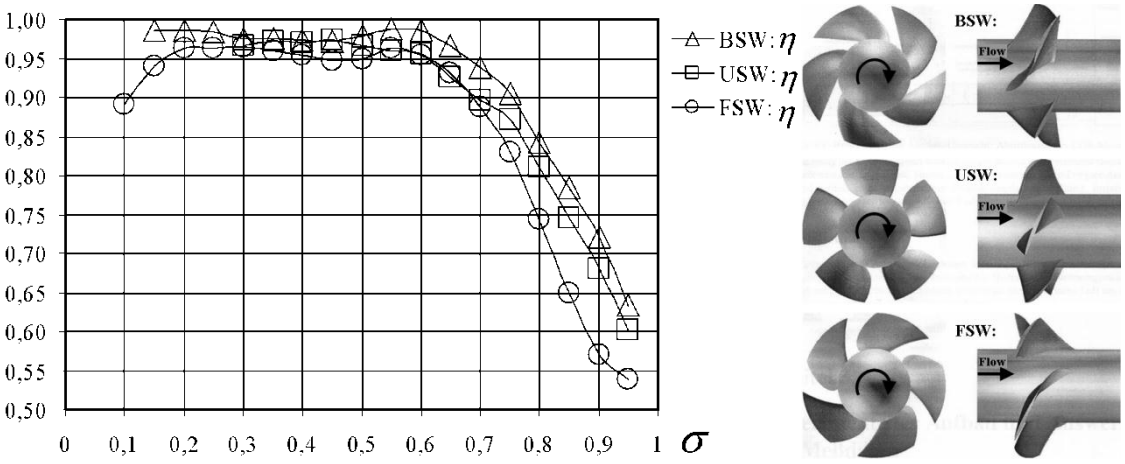

Fig. 3.3. Spanwise distribution of local hydraulic efficiency values calculated from measurement data **[11]**

3.1.2. Secondary losses

The blades and the annulus walls enclose so-called blade passages, in which the streamlines are curved. With action of fluid viscosity, secondary flows are developed, similarly to the 3D secondary flows in pipe bends or elbows (**Fig. 3.4**). The distinction of losses related to such effects from other sources of loss is very complicated. According to the classic view in [2], these effects can be taken into account with use of a secondary loss coefficient, having the following values:

For profiled blading $c_{DS} = 0.018\, c_L^2$ (3.10a)

For cambered plate blading $c_{DS} = 0.025\, c_L^2$ (3.10b)

For the present approach, the secondary loss coefficient is only computed at midspan, and is added in the simplified relationship of $\frac{\Delta p_R{}'}{\Delta p_{tid}}$ (Eq. (3.9)) to c_{Dm}.

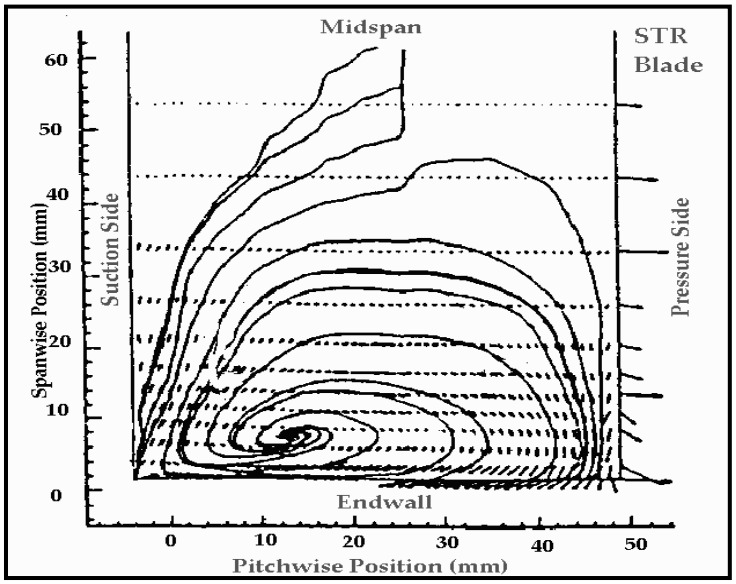

Fig. 3.4. Secondary vortex (passage vortex) detected in the vicinity of the annulus wall of a compressor cascade. Measurement data [13]

According to the classical view, all the 3D flow phenomena causing a departure from the "theoretical" flow of design – e.g. cylindrical stream surfaces – are termed "secondary flows". For example, such a phenomenon is the large-scale vortex developing in the blade passage due to trailing edge shed vorticity, which is due to spanwise changing blade circulation. **Fig. 3.5.**

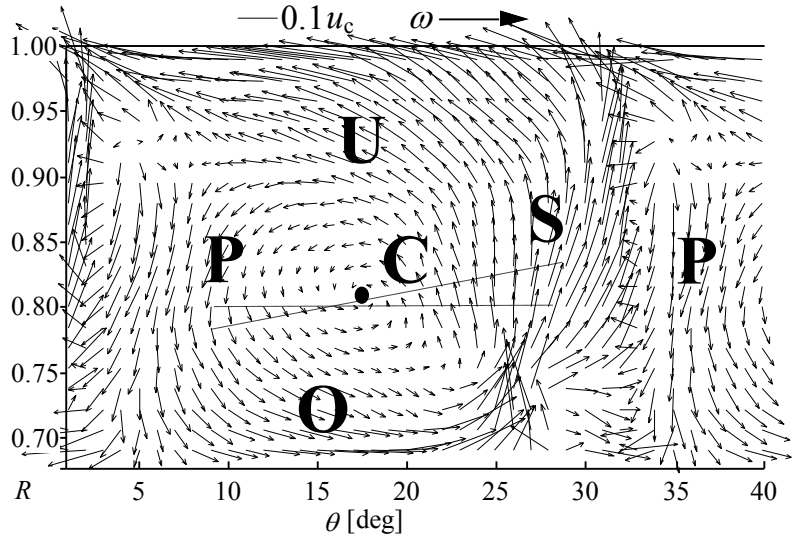

Fig. 3.5. Secondary vector diagram downstream of an axial flow rotor blade passage. Laser Doppler anemometer measurement [14]

The kinetic energy of the "secondary flow" in Fig. 3.5, being dissipated into friction heat, represents a reduction in total stage efficiency in the order of magnitude of some percents.

3.1.3. Annulus losses

The fluid friction appearing on the hub and casing surfaces also results in pressure loss (**Fig. 3.6**). According to former experiences [2], this can be taken into consideration by a constant factor:

Profiled blading: $$\frac{\Delta p_A}{\Delta p_{tid}} = 0.02 \qquad (3.11a)$$

Cambered plate blading: $$\frac{\Delta p_A}{\Delta p_{tid}} = 0.03 \qquad (3.11b)$$

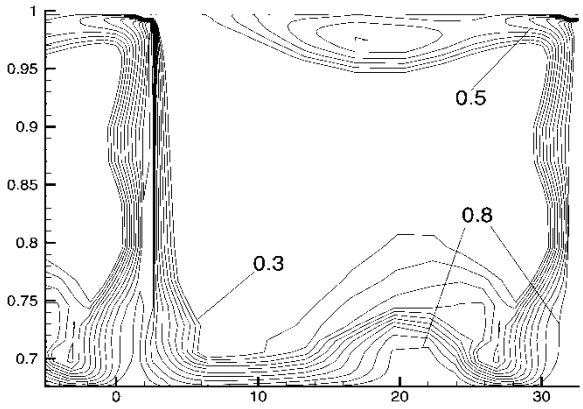

Fig. 3.6. CFD-computed distribution of dimensionless total pressure loss downstream of a rotor blade passage [15]

3.1.4. Tip clearance loss

In the case of axial fans, the tip clearance loss appears as a pressure loss appearing near the casing wall, reducing the hydraulic efficiency. The tip clearance flow, often rolling up into leakage vortex (**Fig. 3.7**), is usually the most significant loss source in modern machinery, also acting as a major noise generator.

According to classic measurement results [2], the losses due to a tip clearance of cca. 1 % blade height have already been taken into consideration in the secondary and annulus losses. Therefore, further clearance losses are expressed as

$$\frac{\Delta p_{CL}}{\Delta p_{tid}} = 2.5\left(\frac{s}{h} - 0.01\right) \qquad (3.12)$$

Where *s* is the size of the clearance, and *h* is the blade height.

Summarising all of the losses related to the rotor, e.g. in the case of profiled blading

$$\frac{\Delta p'}{\Delta p_{tid}} = \frac{w_{\infty m}}{u_m}\frac{1}{\sin(\beta_{\infty m} + \delta)}\frac{c_{Dm} + c_{DS}}{c_{Lm}} + 0.02 + 2.5\left(\frac{s}{h} - 0.01\right) \qquad (3.13)$$

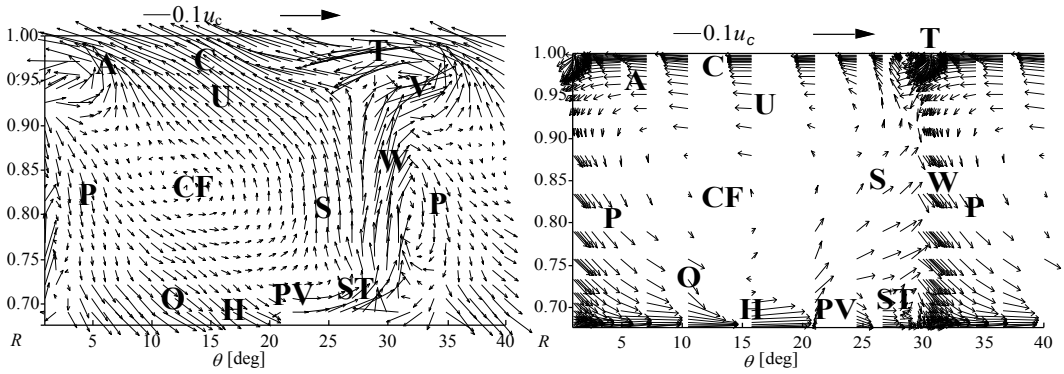

LDA **CFD**

Fig. 3.7. Vector diagram of the secondary flow downstream of an axial flow rotating blade passage. Comparison of Laser Doppler anemometer measurements and CFD computations [16]

3.1.5. Guide vane losses

The stationary guide vane blades also cause losses. Since the relative velocity is considerably lower for guide vanes than in the case of a rotor, their losses are also considerably lower. The guide vane losses comprise profile and secondary losses. Both of them are calculated at midspan. The proposed loss coefficients are as follows:

$$c_{D\,vane} = 0.016 \tag{3.14a}$$

$$c_{D\,vaneS} = 0.018\, c_L^2 \tag{3.14b}$$

These losses usually give cca. 3 % of the overall total pressure rise.

3.1.6. Swirl loss

This kind of loss appears in the case of vaneless rotors, or in the case of guide vaned rotors if they operate off the design point.

This loss is usually cca. 10 % of the ideal total pressure rise. Considering that the guide vanes also have losses, it is understandable that preparation of guide vanes is not economical in the case of fans of moderate performance.

An ideal solution from the viewpoint of elimination of swirl losses is to have two counter-rotating rotors of equal performance – this is the so-called **counter-rotating fan** – ,since by this means the swirl caused by the first rotor is eliminated by the second rotor without guide vanes, and a high performance two-stage machinery is made available. However, such a relatively expensive solution is reasonable only in cases where the pressure rise cannot be realised with a single stage, or other aspects such as **reversibility** are to be taken into account.

3.1.7. Diffuser loss

Two arrangements can be distinguished, with regard to the fluid exiting the axial fan:

a/ The air is transported further on in a duct,

b/ The air exits to the surroundings, or into an enclosure having a cross-section considerably larger than the outlet cross-section.

In case a/, the exit velocity and the annular velocity are to be selected, searching for the most economical solution. A decelerating flow develops between the annulus and the total duct cross-section, the losses of which are to be taken into account.

In order to reduce such losses, a hub diffuser of conical or other streamlined shape is to be applied. In a **pessimistic approach**, the diffuser losses are considered as Borda-Carnot losses [3]. These losses are only significant in the case of a relatively high hub-to-tip ratio.

In case b/, the axial outlet velocity is to be reduced while trying to minimize pressure losses, with the use of an outer diffuser. In order to avoid flow separation at the hub, it is recommended to also apply a hub diffuser extending to the end of the outer diffuser.

For such an arrangement, only the diffuser losses are to be taken into account [2].

If the kinetic energy of the fluid at the end of the diffuser is lost, the sum of the diffuser losses and the outlet losses is to be minimised. For such cases, a diffuser having a smaller efficiency but resulting in a lower outlet velocity may be beneficial.

3.2. Characteristic curve

Based on the velocity triangles, an ideal linear characteristic curve with negative slope can be derived. In this train of thoughts, it is assumed that the shape of the trailing edge determines the outflow direction at any operating point (as for the radial flow machines).

The realistic characteristic curve differs considerably from the ideal one (**Fig. 3.8**). The branch of the characteristic curve having a positive slope frequently appears. Hysteresis is also frequent, which means that the operating point moves along different paths of the characteristic curve when loading or unloading the machine (i.e. increasing and decreasing the volume flow rate). In the catalogues of commercially available axial fans, only the operating ranges of negative slope (i.e. of stable operation) are offered. It is not recommended to operate axial fans at low flow rates, due to the increased noise and unstable operation (surge).

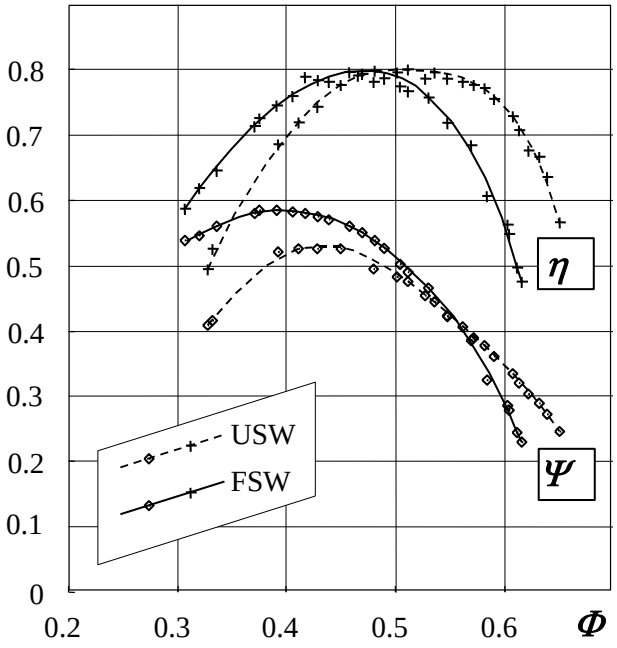

Fig. 3.8. Measured characteristic curves of axial fans of high specific performance: with unswept (USW) and forward-swept (FSW) blades [17]